

## Article

# Combustion Instability and Ash Agglomeration in Wood Pellets Boiler

Lelis Fraga <sup>1,\*</sup>, Eduardo Ferreira <sup>2</sup>, Pedro Ribeiro <sup>2</sup>, Carlos Castro <sup>2</sup> , Jorge Martins <sup>2</sup>  and José C. Teixeira <sup>2,\*</sup> 

<sup>1</sup> Department of Mechanical Engineering, Universidade Nacional Timor Lorosa'e, Rua Formosa 10, Dili 314, Timor-Leste

<sup>2</sup> MEtRICs, Department of Mechanical Engineering, Engineering School, University of Minho, Azurém, 4800-058 Guimarães, Portugal; ef@dem.uminho.pt (E.F.); pedro\_ribeiro@dem.uminho.pt (P.R.); id7607@alunos.uminho.pt (C.C.); jmartins@dem.uminho.pt (J.M.)

\* Correspondence: lelisfraga23@hotmail.com (L.F.); jt@dem.uminho.pt (J.C.T.)

**Abstract:** The combustion instability and ash agglomeration in a wood pellet boiler were investigated in this study. The tests were conducted using the Taguchi method of orthogonal array L<sub>27</sub>(13<sup>3</sup>). Several parameters are applied, including grate area (GA), primary to secondary air split ratio (SR), excess air (EA), and fuel power (P). Pine wood pellets were used, and the boiler's nominal load was 20 kW. The results show that instability during combustion occurs since the fuel bed rises as the accumulation of the unburned wood pellets on the grate causes a slow combustion rate and pressure drop, which creates noise and disturbances. A good combination of the parameters applied to TN9 and TN20 can be useful in obtaining stable combustion. In addition, the ash agglomerations were influenced by the duration of the combustion and the temperature of the fuel bed. The largest size of the ash agglomeration was referred to as test number-TN26 (P: 16 kW, EA: 110%, SR: 30/70, and GA: 115 mm × 75 mm), which is 59 mm, and the duration time is 14,400 s (≈4 h).

**Keywords:** combustion instability; ash agglomeration; wood pellet; boiler



**Citation:** Fraga, L.; Ferreira, E.; Ribeiro, P.; Castro, C.; Martins, J.; Teixeira, J.C. Combustion Instability and Ash Agglomeration in Wood Pellets Boiler. *Energies* **2023**, *16*, 6539. <https://doi.org/10.3390/en16186539>

Academic Editor: Venera Giurcan

Received: 3 August 2023

Revised: 26 August 2023

Accepted: 4 September 2023

Published: 11 September 2023



**Copyright:** © 2023 by the authors. Licensee MDPI, Basel, Switzerland. This article is an open access article distributed under the terms and conditions of the Creative Commons Attribution (CC BY) license (<https://creativecommons.org/licenses/by/4.0/>).

## 1. Introduction

In response to the decreasing use of fossil fuels in the coming years, the development of renewable energy becomes an important issue to be considered [1,2]. Besides being carbon neutral, renewable energy can also contribute to the economic sector, in terms of creating new jobs related to the development of renewable energy [3]. Among renewable energies, biomass is a fascinating and abundant resource to be developed [4]. It shows that of the 14% of global energy supplied by renewable energy sources, more than 70% is composed of biomass [5]. Recent studies focused on the development of biomass resources such as wood [6,7], wood pellets [8], wood particles [9,10], waste [4,6], etc. In addition, biomass and renewable waste are apparently the main energy sources, whose share will increase in the future [11].

Besides being environmentally friendly, biomass also releases gases into the environment through combustion. Among the gas emissions, such as CO, CO<sub>2</sub>, CH<sub>4</sub>, NO<sub>x</sub>, etc., produced through incomplete combustion [12], solid emissions will also be produced, such as ashes and particulate matter (PM) [13,14]. The complete combustion indicates less CO emission [15,16] and, less ashes and PM [17]. Complete combustion is indicated by good mixing and enough residence time at high temperatures [15].

The emission has an adverse impact during the combustion process, including reduced combustion efficiency [18]. This emission will also deteriorate the equipment and increase the operational cost as a result of the corrosiveness and melting [6,18,19]. Among their impacts on the equipment, the pollution from the atmospheric aerosols and ambient PM is considered of great concern as it has a serious impact on human health and, related to aerosol exposure, has garnered much research attention in the fields of epidemiology and

toxicology [20]. The main elements in the biomass ash, as described by Magdziarz et al. [4] are potassium, calcium, sulfur, chlorine, silicon, and phosphorus. The study conducted by Chlebnikovas et al. [11] on using various blends of biofuel containing lignin for heat production and emissions to the air during combustion processes reveals that, in contrast to pure lignin, the concentrations of alkali metals, boron and, to a lesser extent, nickel and chlorine have increased the most in bottom ash.

Several studies have been conducted on improving the biomass combustion in a furnace by minimizing the problems that occur during the combustion, such as ashes. The problems caused by the slagging and fouling of ash include reduced heat transfer, corrosion and erosion problems, and an increased probability of shutdown for maintenance and cleaning [2]. In reducing the ash formation during combustion, adding the additive is one method, along with fuel mixing and leaching out the problematic elements from fuels before combustion [21]. The authors revealed that the additive utilization will influence the chemical binding as the most important effect to convert problematic ash elements into high-temperature stable substances.

Wang et al. [22] investigated the slagging and fouling and elemental constituents of straw/woody biomass from wheat straw, cotton straw, and sawdust. This study revealed a high deposition and corrosion risk from these biomass applications. The slagging and fouling in biomass co-combustion were also investigated by Tortosa-Masiá et al. [19]. This study referred to the influence of deposition formation on the heat transfer in the heat exchanger. The gas emissions and ashes from raw residue materials and the different types of pellets were investigated by Ferreira et al. [6]. This study shows that the co-combustion of shoemaking, textiles, and plastics residues does not reflect the concentration limits for CO. Besides, the problem also occurred regarding the high tendency of ash slagging.

The effect of excess air ratio on the combustion of switchgrass and hardwood was investigated, and the fouling and slagging tendencies of their ash were evaluated by Wang et al. [23]. This study used different excess air ratios (EAR) from 1.0–1.3 or 0–30% of excess air, which indicated that a different EAR has an influence on the ash and char, and hardwood combustion produced fewer residues (ash and char by weight) than switchgrass. Meanwhile, increasing the EAR produces more complete combustion and reduces the amount of unburned residue. The study on the particle formation mechanisms and the influence of different operating parameters on the particle emissions in wood pellets combustion under fixed-bed conditions was conducted by Wiinikka and Gebart [24]. This study describes that the particles released from this combustion are formed in three different mechanisms namely coarse fly ash particles ( $>10\ \mu\text{m}$ ), submicrometer-sized fly ash particles, and, submicrometer-sized soot particles. These different particles are produced from mechanical ejection from the fuel bed, the vaporization and nucleation of ash minerals, and incomplete combustion respectively.

Slagging tendencies of wood pellet ash in residential pellet burners were investigated by Öhman et al. [25]. Several parameters were investigated, including the effect of the different raw materials for pellets affect the accessibility of the burner equipment, the ash forming elements that are responsible for the deposit or slag formation, and the critical slag temperature for the different raw materials. This study revealed that the amounts of ash deposits produced were affected both by the burner and the fuel types used. In addition, the Si-content in the fuel correlated well with the sintering tendencies in the burners. Study on effect of biofuel type, ignition technique, biomass load, cleavage, and secondary air supply on chemical composition of particulate matter emissions in a woodstove was conducted by Vicente et al. [17]. Pine softwood and beech hardwood was used. This study revealed that the Organic Carbon content of  $\text{PM}_{10}$  was higher when higher loads were fed into the combustion chamber. Different wood pellet boiler and operational load, and different burner configuration was investigated by Verma et al. [26]. This study revealed that at low load, the top feed boiler had very high dust emissions ( $406.4\ \text{mg Nm}^{-3}$ ), this value was 17.6 times higher than at nominal load.

The chemical composition and melting behaviors of ashes from *Pinus Sylvestris* forest biomass were studied by Dibdiakova et al. [7]. This study shows that from the combustion of pine trees, the chemical composition of the ashes was mostly composed of Ca, K, Mg, Mn, P, and Si. Besides, the melting process of the ashes started in the temperature range of 930–965 °C. The experimental study on the ash fusion characteristics of biomass red pine, corn straw, Bermuda grass, and bamboo was investigated by Fang and Jia [2]. This revealed that among the other biomasses, the ash deformation temperatures of pine and straw are over 1100 °C. The physicochemical properties of biomass, including rice straw, pine sawdust, and Chinese Parasol Tree leaf burned, were investigated at different ash temperatures (815 °C, 600 °C and 500 °C). This study presented that the ash content, composition, crystalline phase composition, surface morphology, and ash fusibility were all closely related to ash temperatures [27].

An investigation on the combustion of pellets of pine, industrial wood wastes, and peach stones in a domestic boiler was conducted by Rabaçal et al. [8] and evaluated the combustion and its emission characteristics. This study shows that the pine pellets have a high tendency to cause fouling and slagging. The characterization of the biomass and sewage sludge ashes and their impact on fouling and slagging during combustion were studied by Magdziarz et al. [4]. This study revealed that the ash composition determines the slagging, fouling, and corrosion risks in biomass and sewage sludge combustion. Various biomass fuels, including pine wood and coal combustion in a wood and pellet stove was investigated by Fachinger et al. [28]. The emission factors for various gaseous and particulate pollutants based on burning phase, burning condition, and fuel were observed. This study revealed that at very low and very high burn rates, combustion efficiency was found to be low, while no significant differences were found for the emissions from different wood species. The effect of biomass raw materials from softwood stem, bark, and peat on particle and gaseous emissions and ash behavior was studied by Sippula et al. [14]. This study was conducted in a 500 kW of reciprocating grate boiler, where the primary air was supplied through grate elements and the secondary air was supplied above the fuel bed.

Combustion instability is an important issue in combustion processes. Biryukov [29] stated that flame instability is determined by the influence of both transport processes on the flame or diffusion-thermal processes, depending on its structure, and hydrodynamic processes, as an example the effects of gas flow. Combustion instability is also defined as an unstable feedback configuration of a thermoacoustic process driven by a fluctuated heat release rate and a resulting velocity fluctuation, and a combustion process whose heat fluctuation is affected by a surrounding velocity fluctuation [30]. In addition, combustion instability shows in the increasing of pressure and velocity fluctuations as time goes. In combustion processes, the dynamic instability occurs which is due to the feedback coupling between two dominant processes, acoustics and heat release, and is referred to as thermoacoustic instability [31].

Agglomeration of the ashes in the combustion of solid fuel is important to analyze in order to understand the behavior and its effect on the apparatus. In addition, the combustion instability has an important effect in relation with the stability and safe operation of a wood pellet boiler. The objective of this study is to investigate the combustion instability and of ash agglomeration from wood pellets combustion in a small scale boiler with different thermal load, excess air, split ratio of primary to secondary air, and grate size.

## 2. Materials and Methods

### 2.1. Study Method

This research was conducted at the Laboratory of Energy and Fluids, School of Engineering, University of Minho, Portugal. As this is another part of the previous research conducted by the same authors [32]. The schematic diagram of the test facility used in this study is presented in Figure 1. It consists of: the boiler unit (including heat exchanger pipes, combustion chamber and fuel grate), the ventilator, fuel storage, external cooling loop, the gas analyzer unit and computer and the data acquisition unit. The fuel is transported

from the fuel storage tank by means of screw and is supplied on top of the combustion chamber by gravity. The ventilator drafts the air into the combustion chamber by primary and secondary air pipes working below atmospheric pressure. A vacuum pump was used to extract a sample of exhaust gas into the gas analyzer for measurement purposes. Before entering the vacuum pump, the sample was cooled and filtered in order to remove any moisture and particles. The computer unit, including a National Instrument data acquisition board, was used to monitor and control all the systems. The boiler condition can be seen in Castro et al. [32]. In order to describe the combustion instability by emissions, the exhaust gases were also measured, including CO (13% of O<sub>2</sub>), O<sub>2</sub>, and CO<sub>2</sub> in the chimney by a “Multi gas analyzer 9000” and NO<sub>x</sub> by a “NO<sub>x</sub> gas analyzer”. The gas analyzer was calibrated before starting the measurement by pressing the automatic calibration button. Several points of temperature on the boiler were also measured.

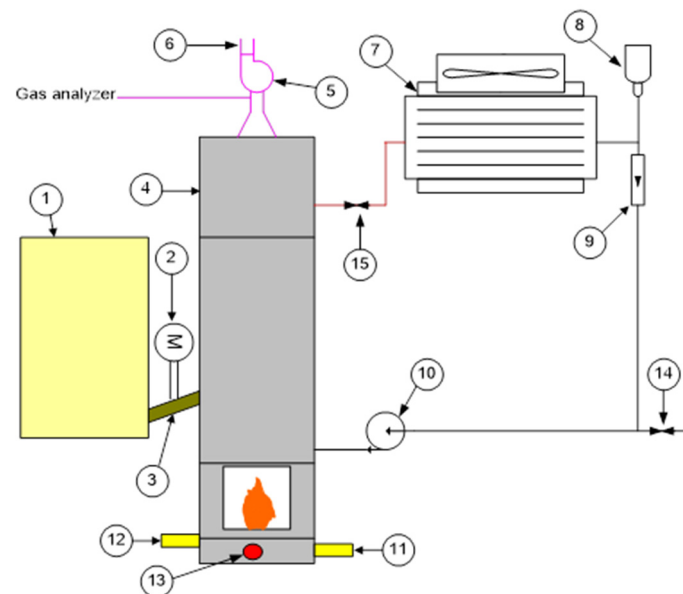


**Figure 1.** Experimental diagram: 1. Pellets storage tank, 2. Feeding motor, 3. Feed auger, 4. Boiler, 5. Ventilator, 6. Stack, 7. Air cooler heat exchanger, 8. Expansion vessel, 9. Flow meter, 10. Water pump, 11. Primary air tube, 12. Secondary air tube, 13. Ignition coil, 14. Water inlet valve and 15. Hot water outlet valve.

The total air flow rate is set by adjusting the ventilator draft and the primary/secondary air split is adjusted by throttling the primary air supply. The whole unit is covered by a jacket of rock wool to minimize the heat losses on the outside. The grate is installed underneath the combustion chamber and locked into place by screws. The grate is covered by the metal box and a sealing material (rock wool) was applied to the connection parts to prevent uncontrolled air entry on those parts during operation. The primary air pipe is installed underneath and the secondary air is installed above the grate. The ignition coil is in the front of the grate box and the fuel inlet is on the top of the grate. The grate applied in this study was of a rectangular shape that can be seen in the previous paper [32], can be easily changed and three different cross sections, areas according to the study were used. The grate model is schematically described in Figure 2, where 1 and 4 are primary and secondary air orifices (4 mm diameter) respectively, 2 is the primary air orifice on the bottom (3 mm width), 3 is the ignition hole and 5 is the secondary air inlet.

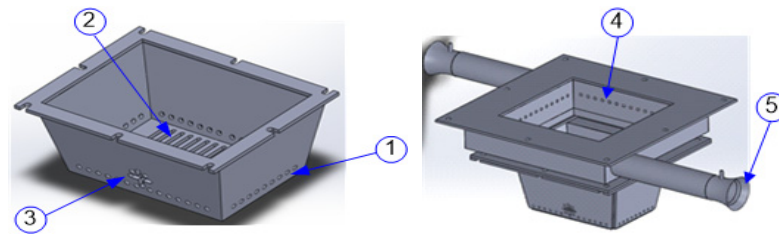


**Figure 2.** Grate unit [32]: (1) Primary air orifices, (2), Primary air orifices on the bottom, (3) Ignition hole, (4) Secondary air orifices and (5) Secondary air inlet.

The suction ventilator (working frequency between 0–60 Hz) was installed in the exhaust duct to draft the air into the grate through primary and secondary air pipes, and also to release the exhaust through the stack. The thermal load is removed from the boiler through a cooling loop. In this, a circulating pump (maximum flow rate of 500 L/h) drives the cooling water through an air-cooled heat exchanger and back to the boiler. The flow rate is controlled by a valve and measured by a calibrated rotameter. The parameters applied in this study include power, excess air, a split ratio of primary to secondary air, and grate area at three different levels, including grate height ( $h$ ) as shown in Tables 1 and 2 respectively.

**Table 1.** Study parameters.

No.	Power (kW)	Mass Fuel (kg/h)	Total Mass of Air (kg/h) and $\lambda$			PA:SA
			1.5	1.7	2.1	
1	10	2.11	18.52	20.94	25.86	20:80
2	13	2.74	24.02	27.22	33.62	30:70
3	16	3.37	29.56	33.50	41.38	37:63

**Table 2.** Grate size.

No.	Size (mm $\times$ mm)	$h$ (mm)
1	90 $\times$ 75	61
2	115 $\times$ 75	
3	115 $\times$ 96	

## 2.2. Study Material

The pine wood pellets certified according to the ENPlus standard, which is rated as A1 class pellets, were used in this study [33]. The full interval of each parameter from the entire mass of fuel that is used are summarized in Table 3 [34].

## 2.3. Data Collection

The data referring to instability combustion and ash agglomeration were observed and recorded for each 27 experiments. The instability can be identified through observation of the fuel bed and rising temperature, noise and the increasing increase in CO emissions. Meanwhile, the results presented in this paper are referred to the test with the instabilities conditions. The ashes were collected from three different locations, including inside the grate, on the top of the grate and on the wall of the chamber. The ashes are composed of some small to large particles. Based on the formation of ashes collected, they then measured with ImageJ software to identify their sizes. Within the ImageJ software, we set the scale of the distance from pixel to centimeter with a pixel aspect ratio of 1.

**Table 3.** Properties of pine wood pellets [34].

Proximate Analysis (wt.%, as Received)		Ultimate Analysis (wt.%, Dry Ash Free)	
Moisture	6.9	Carbon	50.8
Volatile matter	77.80	Hydrogen	5.39
Ash	0.6	Nitrogen	1.55
Fixed carbon	14.70	Sulphur	0.037
Lower Heating Value (MJ/kg)	17.1	Oxygen	42.22
Other parameters			
Cl (%)	0.001	Fe (%)	0.023
Cr (%)	0.004	K (%)	0.067
Cu (%)	0.002	Na (%)	0.01
Mn (%)	0.011	Si (%)	0.043
Ni (%)	0.004	P (%)	0.014
Al (%)	0.033	Ti (%)	0.002

### 3. Results and Discussion

#### 3.1. Emission Characteristics

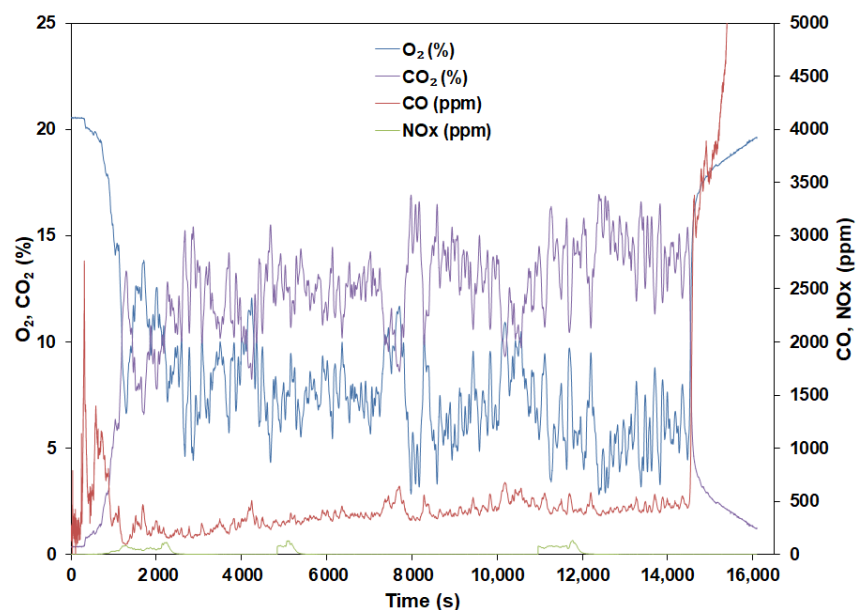
Emissions were measured automatically in the chimney by a “Multi gas analyzer 9000” (CO, O<sub>2</sub>, and CO<sub>2</sub>), and NO<sub>x</sub> by a “NO<sub>x</sub> gas analyzer”. The volatile fuels from the bed combustion are assumed to be light hydrocarbons (modelled as methane), heavy hydrocarbon (tar modelled as C<sub>x</sub>H<sub>y</sub>), carbon monoxide (CO) and hydrogen (H<sub>2</sub>). In addition, the effluent gases also include: H<sub>2</sub>O and N<sub>2</sub> [35]. Figure 3 shows, as an example, the gas emissions during a run at 13 kW with the excess air of 70%, the P/S split ratio of 37/63 and a grate area 115 mm × 96 mm, referred to as test number 15 (TN15). The input parameter and the average value of gas emission and temperature in the fuel bed recorded are presented in Tables 4 and 5. The rising of fuel beds means that the feeding rate of wood pellets is unbalanced by the mass loss rate. This leads to the fuel bed increasing gradually up to 60 mm or overflowing the grate. After the fuel bed rises, the combustion becomes unstable, which is followed by an increase in CO emissions. The thermal efficiency of the boiler obtained for TN15 was 91.77%, with the cold and hot water temperature on the heat exchanger being 36 °C and 68 °C respectively. As shown in Figure 3, all gases were measured continuously, except for NO<sub>x</sub> which was measured within about 12–15 min during the test. In this study, the emissions fluctuate due to several conditions such as temperature, the gas residence time (ratio of volume of the combustion chamber/gas flow), turbulence and excess air, which are decisive for the optimization of the combustion process [36].

**Table 4.** The input parameter for TN15.

Parameter	Value
T ambient (°C)	19
Fuel flow rate (kg/h)	2.75
Primary air flow rate (m <sup>3</sup> /h)	8.11
Secondary air flow rate (m <sup>3</sup> /h)	14.06

**Table 5.** The experimental data for TN15.

Parameter	Before FB Rising	After FB Rising	Overall	T <sub>fb</sub> (°C)
O <sub>2</sub>			8.29%	627 (5 mm)
CO (13% O <sub>2</sub> )	262 ppm	427 ppm	390 ppm	913 (15 mm)
NO <sub>x</sub>			70 ppm	866 (25 mm)
CO <sub>2</sub>			12.93%	542 (60 mm)

**Figure 3.** Gas emissions profiles for TN15.

### 3.2. Combustion Instability

During the course of the various tests, it was observed that instabilities could occur over the long run. These were identified with a sudden rise in the fuel bed height that would lead to an increase in emissions and, ultimately, to a collapse of the combustion. This is a reason why boiler manufacturers introduced a control strategy that, periodically, cleans the fuel bed. Table 6 presents the experimental and a qualitative assessment of the combustion behavior for the 27 tests. In the table  $t_{av,ins}$  is the average time (moment) when the instability starts to occur and  $t_{run}$  is the running time (duration of the test). The data in Table 6 shows that the majority of the experiments experienced instability which is indicated by the fuel bed rising and increase in CO emissions. The instability occurs as an indication of the poor combination of the parameters applied which results in a high CO concentration as referred to TN1 and TN3 (see Figure 4). The left side is the temperature profile and the right side is the emission profile. The instability is mostly linked to the fuel bed rising, which may be a consequence of the lower combustion rate (accumulation of unburned pellets in the grate). The instability may also occur as a result of the poor combination of the parameters applied, which is referred mostly to the GA.

**Table 6.** Stability and instability combustion condition of the experiment identified.

Test.	P (kW)	EA (%)	GA (mm <sup>2</sup> )	SR	t <sub>av,ins</sub> (s)	t <sub>run</sub> (s)	Indication	CO after FB Rising (ppm)	Description
TN1	10	50	90 × 75	20/80	2300	4500	High CO	1830	Poor combustion: Instability, FB rising, and condensation.
TN2	10	50	115 × 75	30/70	3600	5500	Fuel bed rising	217	Instability and condensation.
TN3	10	50	115 × 96	37/63	2500	4500	High CO	1985	Poor combustion: high CO, noisy, flame instability and condensation.
TN4	10	70	90 × 75	30/70	3500	5500	Fuel bed rising	334	Instability.
TN5	10	70	115 × 75	37/63	6600	8900	Fuel bed rising	847	Noise and condensation.
TN6	10	70	115 × 96	20/80	4500	6000	Fuel bed rising	470	Instability and condensation.
TN7	10	110	90 × 75	37/63	8600	14,400	Fuel bed rising	561	Instability and condensation.
TN8	10	110	115 × 75	20/80	5000	14,400	Fuel bed rising	282	Instability, noise and condensation.
TN9	10	110	115 × 96	30/70	14,400	14,400	-	415	Stable combustion.
TN10	13	50	90 × 75	37/63	2700	5000	Fuel bed rising	149	Instability and condensation.
TN11	13	50	115 × 75	20/80	3200	5400	Fuel bed rising	787	Instability and condensation.
TN12	13	50	115 × 96	30/70	6500	9000	Fuel bed rising	176	Instability and noise.
TN13	13	70	90 × 75	20/80	2800	10,000	Fuel bed rising	262	Instability and condensation.
TN14	13	70	115 × 75	30/70	5400	12,000	Fuel bed rising	490	Instability.
TN15	13	70	115 × 96	37/63	14,400	14,400	Fuel bed rising	427	Noise.
TN16	13	110	90 × 75	30/70	3100	7500	Fuel bed rising	218	Instability.
TN17	13	110	115 × 75	37/63	6000	14,400	Fuel bed rising	213	Small instability.
TN18	13	110	115 × 96	20/80	7200	14,400	Fuel bed rising	395	Noise.
TN19	16	50	90 × 75	30/70	2900	6100	Fuel bed rising	246	Instability.
TN20	16	50	115 × 75	37/63	14,400	14,400	-	212	Stable combustion.
TN21	16	50	115 × 96	20/80	5800	14,400	Fuel bed rising	350	Small instability.
TN22	16	70	90 × 75	37/63	5200	8000	Fuel bed rising	413	Instability and noise.
TN23	16	70	115 × 75	20/80	4100	11,000	Fuel bed rising	242	Small instability.
TN24	16	70	115 × 96	30/70	8000	14,400	Fuel bed rising	325	Small instability.
TN25	16	110	90 × 75	20/80	2400	6000	Fuel bed rising	341	Instability.
TN26	16	110	115 × 75	30/70	7400	14,400	Fuel bed rising	492	Instability.
TN27	16	110	115 × 96	37/63	14,400	14,400	-	544	Small noise.

The instability may be identified in some cases from a phenomenon such as noise, the increase of CO emissions, and the increasing of the fuel bed in which can be observed directly or from the increasing of the temperature at 60 mm above the fuel bed. The noise occurs as a result of vortex generation (associated with a higher pressure drop) and oscillation in the air flow rate. This may result from the accumulation of pellets on the grate which blocks the primary air entrance or also a larger GA that may create a low velocity of the primary air flow through the grate. Yazdanpanah et al. [37] stated that the pressure drop is caused by pellet size, geometry of container cross-section, and air flow rate. The authors revealed that pressure drop increases with the air flow rate and smaller wood pellets. Regarding the geometry of the container cross-section, Ray et al. [38] stated that the pressure drop increases with a packed fill versus a loose fill.

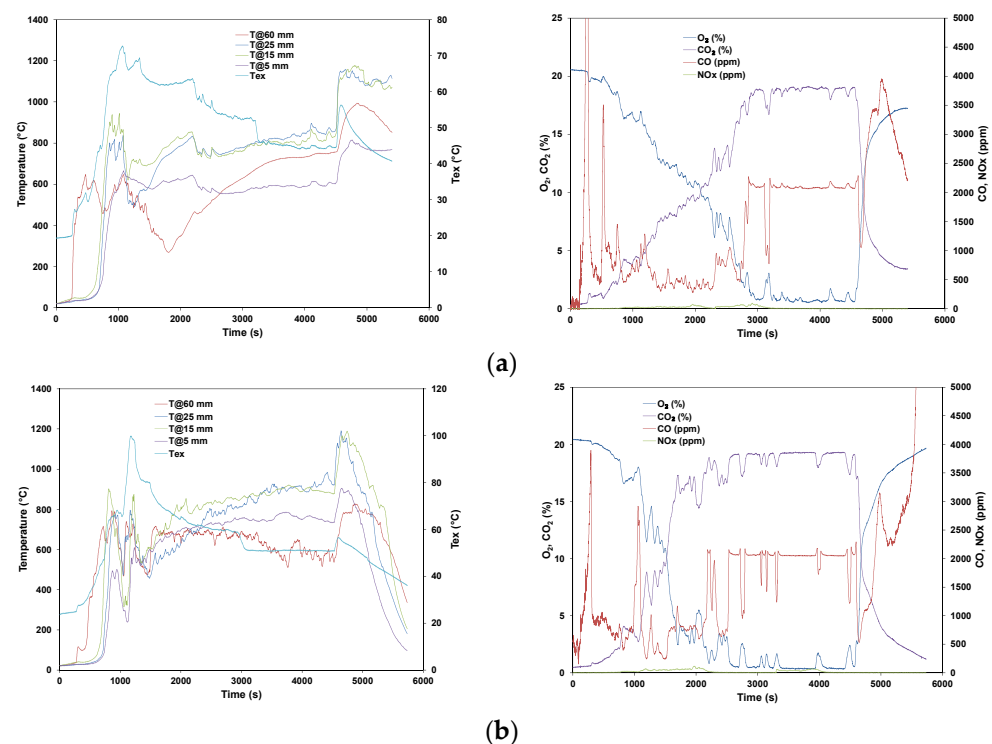


**Figure 4.** Temperature and emissions profiles for (a) TN1, and (b) TN3.

Condensation is an indication of the dropping of the exhaust temperature (the profile of the exhaust temperature can be seen in the figure for temperature profile, even though, among those experiments, TN9 and TN20 are considered as stable combustion examples since there was no indication of instability during the 4 h running (see Figure 5). This is an indication of the good combination of parameters applied in this study. In general, from the instability data and the resulting data, one can conclude that the middle size grate is the optimum grate. Meanwhile, Figure 6a shows that after the fuel bed rose (as indicated by the temperature profile in 60 mm) the experiment was terminated because the instability was very high, which is coupled with a sharp increase of CO. However, as illustrated by Figure 6b one test was extended for 4 h because the system shifted to another stable condition.

The instability of exhaust temperature can result from poor combustion in the grate that produces low temperature (see Figure 6a). However, the increasing in the exhaust temperature may relate to the higher air flow rate (higher EA) that may expel more heat to the exhaust pipe (see Figure 7a). The same condition may also be obtained for SR, as increasing the SR contributes to the increasing of the exhaust temperature (e.g., see Figure 7b test at 70% of EA and at a middle SR).

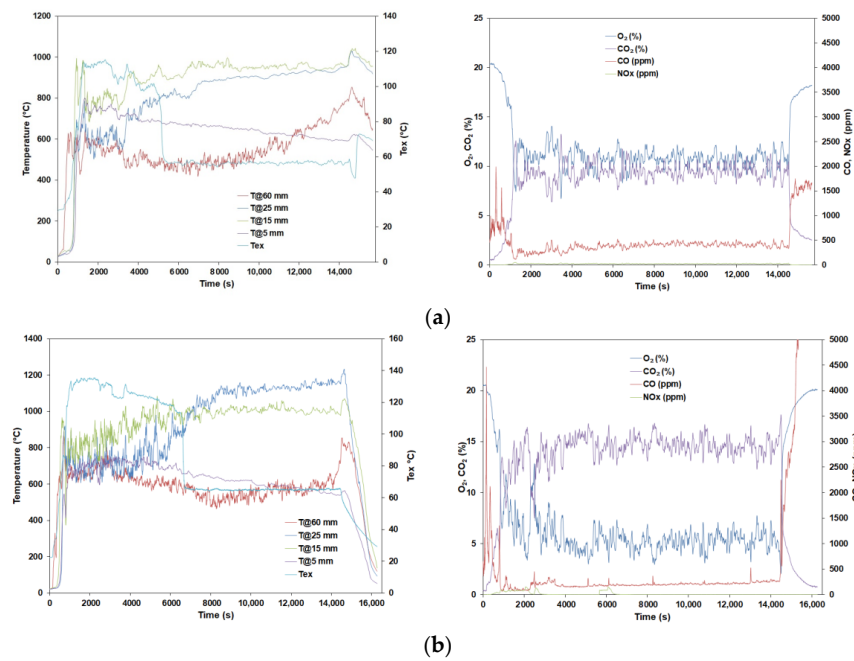


Figure 5. Temperature and emissions profiles for (a) TN9, and (b) TN20.

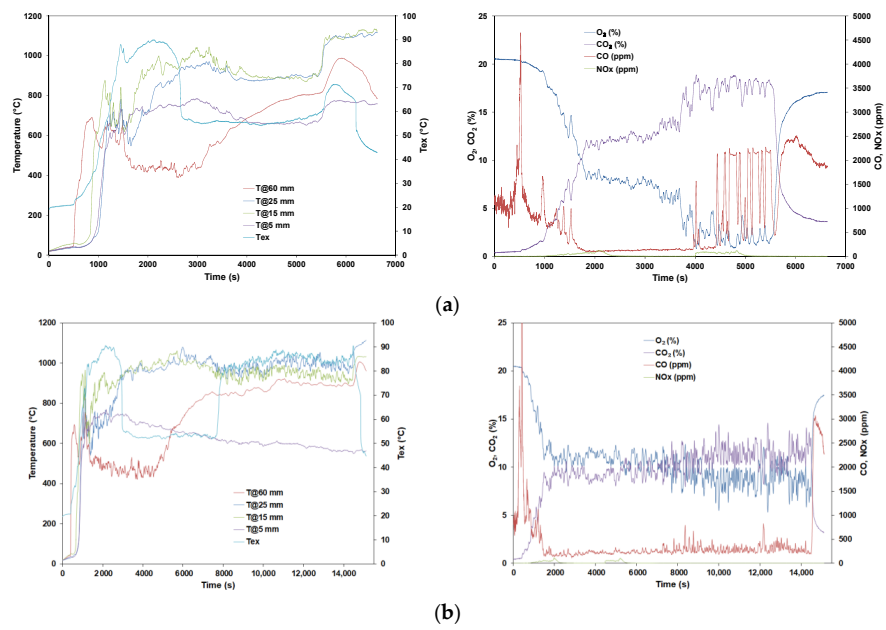


Figure 6. Temperature and emissions profiles for (a) TN11, and (b) TN8.

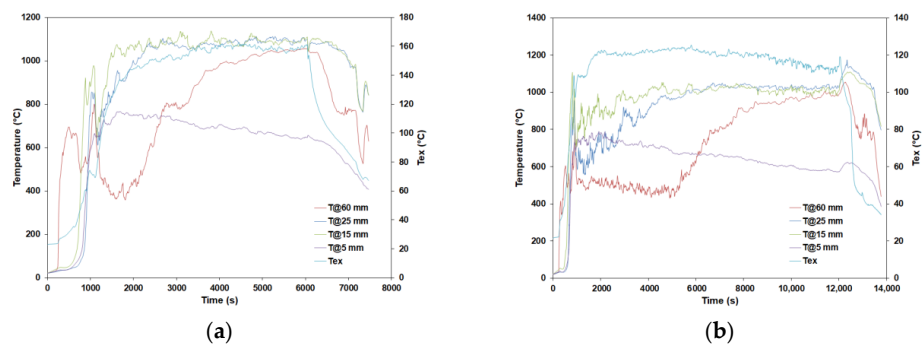


Figure 7. Temperature profiles for (a) TN25, and (b) TN14.

Figure 8 shows that the shorter the instability time ( $t_{av,ins}$ ), the earlier the instability was observed and when  $t_{av,ins} = t_{run}$  means there is no instability (fuel bed rising) during the combustion of the wood pellets (e.g., TN9, TN20, and TN27). Figure 8a–c shows that in a certain combination of power, EA and GA create an early instability, such as a small GA with a middle or higher power and a lower EA (e.g., TN10 and TN19, see Figure 9). Meanwhile, the SR ratio has no significant influence on instability since the same trend was observed for different SR.

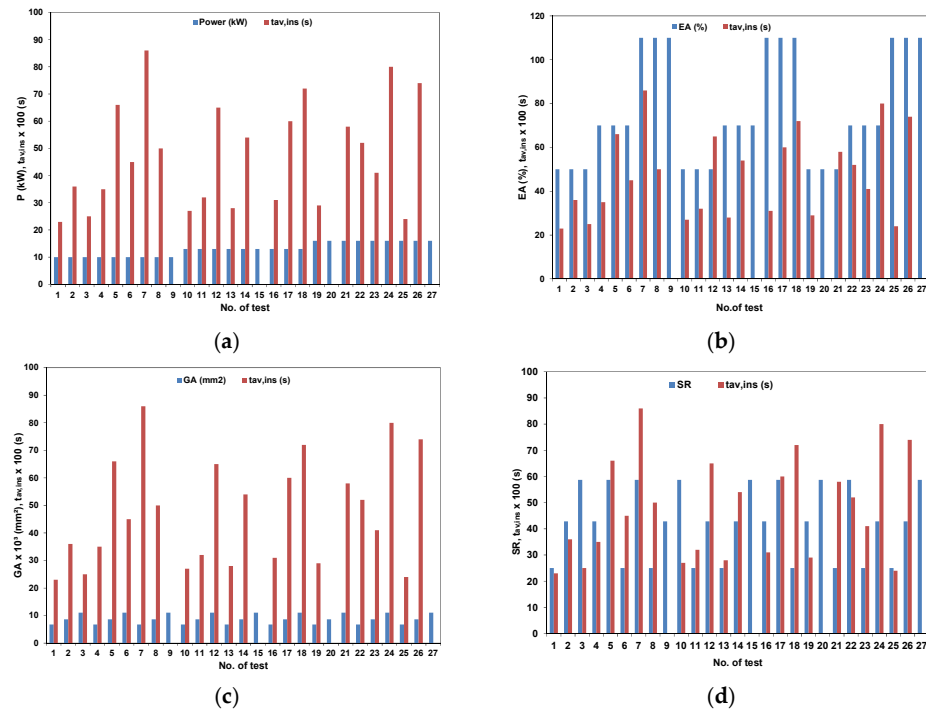


Figure 8. Combustion characteristics on the instability: (a) Power (kW) vs. instability time (s), (b) EA (%) vs. instability time (s), (c) GA (mm<sup>2</sup>) vs. instability time (s) and (d) SR vs. instability time (s).

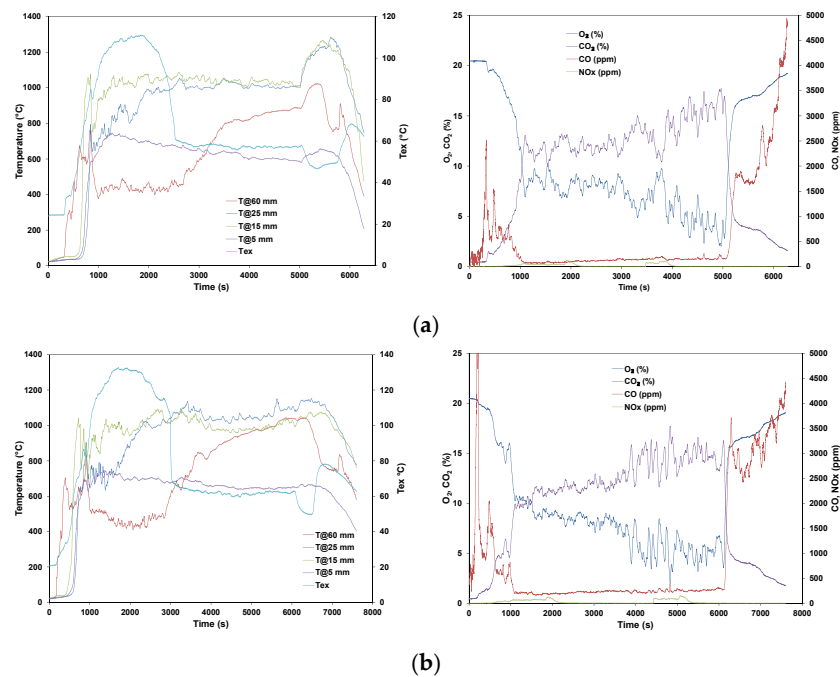


Figure 9. Combustion characteristics on the instability (a) TN10, and (b) TN19.

### 3.3. Ashes Formation and Agglomeration

Subsequently, for each experimental run, the ashes were collected from the bottom of the grate. A high resolution frame was collected, and the ImageJ software was used to measure the size of the aggregated ashes. They were measured based on the larger size of its agglomeration. Generally speaking, ash formation and agglomeration depend upon the burner and fuel types [25]. It was observed that the agglomeration of the ashes occurred when the boiler was operated at a high load and high-temperature condition [39]. Dibdiakova et al. [7] reveal that the chemical composition of the ashes from the combustion of a pine tree contains mostly Ca, K, Mg, Mn, P, and Si, and the melting process of the ashes started in the temperature range of 930–965 °C. For red pine, the ash deformation temperatures are over 1100 °C [2]. In addition, the remaining mass is fixed carbon and ashes, or unburned substances, after the combustion of these wood pellets is about 3%. This result refers to a previous study regarding the mass loss of wood pellets [40].

This study also revealed that, besides several conditions mentioned before that have an influence on ash agglomeration, the duration of the combustion is also determinant for the agglomeration of the ashes. For example, the combustion of pine wood pellets with TN2 (10 kW, EA 50%, and SR 30/70) with a duration time of 5500 s has almost no agglomeration above 3 mm in size, but only shows their sintering (see Figure 10a). The degree of sintering is mostly an effect of the composition of the fuel ash [41]. Moreover, when the time of the combustion is less than 5500 s, the ash agglomeration is less than 10 mm in size. Incidentally, the largest size of the ashes agglomeration was referred to TN26 (16 kW, EA 110%, and SR 30/70) which is 59 mm and the duration time is 14,400 s ( $\approx 4$  h), see Figure 10b. Other experimental data on the agglomeration of ash under different combustion times with their observation is presented in Table 7.

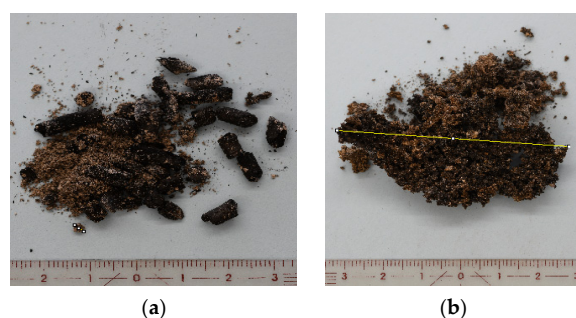


Figure 10. Ash agglomeration, (a) TN2 and (b) TN26.

Table 7. Experimental data on the agglomeration of ash under different combustion times.

No.	Figure	Time (s)	Observation	No.	Figure	Time (s)	Observation
TN1		4500	The large ash agglomeration is 7 mm, and the residue is composed of some ashes and char.	TN15		14,400	The large ash agglomeration is 28 mm, and the residue is composed of some ashes and almost no char.
TN2		5500	The large ash agglomeration is 3 mm, and the residue is composed of some ashes and char.	TN16		7500	The large ash agglomeration is 28 mm, and the residue is composed of some ashes and a few chars.

Table 7. Cont.

No.	Figure	Time (s)	Observation	No.	Figure	Time (s)	Observation
TN3		4600	The large ash agglomeration is 10 mm, and the residue is composed of some ashes and almost no char.	TN17		14,400	The large ash agglomeration is 20 mm, and the residue is composed of some ashes and a few chars.
TN4		5500	The large ash agglomeration is 6 mm, and the residue is composed of some ashes and char.	TN18		14,400	The large ash agglomeration is 12 mm, and the residue is composed of some ashes and a few chars.
TN5		9000	The large ash agglomeration is 17 mm, and the residue is composed of some ashes and almost no char.	TN19		6000	The large ash agglomeration is 12 mm, and the residue is composed of some ashes and a few chars.
TN6		6000	The large ash agglomeration is 3 mm, and the residue is composed of some ashes and char.	TN20		14,400	The large ash agglomeration is 32 mm, and the residue is composed of some ashes and a few chars.
TN7		14,400	The large ash agglomeration is 17 mm, and the residue is composed of some ashes and a few chars.	TN21		14,400	The large ash agglomeration is 20 mm, and the residue are composed of some ashes and with almost no char.
TN8		14,400	The large ash agglomeration is 4 mm, and the residue is composed of some ashes and char.	TN22		8000	The large ash agglomeration is 25 mm, and the residue is composed of some ashes and almost no char.
TN9		14,400	The large ash agglomeration is 47 mm, and the residue is composed of some ashes and char.	TN23		11,000	The large ash agglomeration is 24 mm, and the residue is composed of some ashes and almost no char.

Table 7. Cont.

No.	Figure	Time (s)	Observation	No.	Figure	Time (s)	Observation
TN10		5000	The large ash agglomeration is 7 mm, and the residue is composed of some ashes and almost no char.	TN24		14,400	The large ash agglomeration is 17 mm, and the residue is composed of some ashes and a few chars.
TN11		5600	The large ash agglomeration is 10 mm, and the residue is composed of some ashes and a few chars.	TN25		6000	The large ash agglomeration is 10 mm, and the residue is composed of some ashes and a few chars.
TN12		14,400	The large ash agglomeration is 6 mm, and the residue is composed of some ashes and a few chars.	TN26		14,400	The large ash agglomeration is 59 mm, and the residue is composed of some ashes and almost no char.
TN13		10,000	The large ash agglomeration is 7 mm, and the residue is composed of some ashes and a few chars.	TN27		14,400	The large ash agglomeration is 10 mm, and the residue is composed of some ashes and almost no char.
TN14		12,000	The large ash agglomeration is 23 mm, and the residue is composed of some ashes and char.				

Figure 11a–d shows that from the parameters applied (P, EA, GA, and SR) the middle and higher levels tend to increase the ash accumulation size. The high fuel bed temperature and long running time have also increased the ash accumulation size (see Figure 11e,f). The longer residence time (longer running of the boiler) of wood pellet combustion also produces more ash agglomeration. These conditions indicate that the agglomeration of the ashes is a function of time and temperature. In addition, Ribeiro et al. [42] also stated that the ash agglomeration is mostly related to the changing of the chemical elements ratio due to vaporization of the more volatile species. Figure 11a–f shows that the longest ash agglomeration size was observed for test TN26 with combination parameters including higher power (16 kW) and EA (110%) but at a middle GA (115 mm × 75 mm) and SR (30/70). Then, following the ash agglomeration size observed for test TN9, a combination parameter was included: lower power (10 kW) and middle SR (30/70), but at a higher EA (110%) and GA (115 mm × 78 mm).

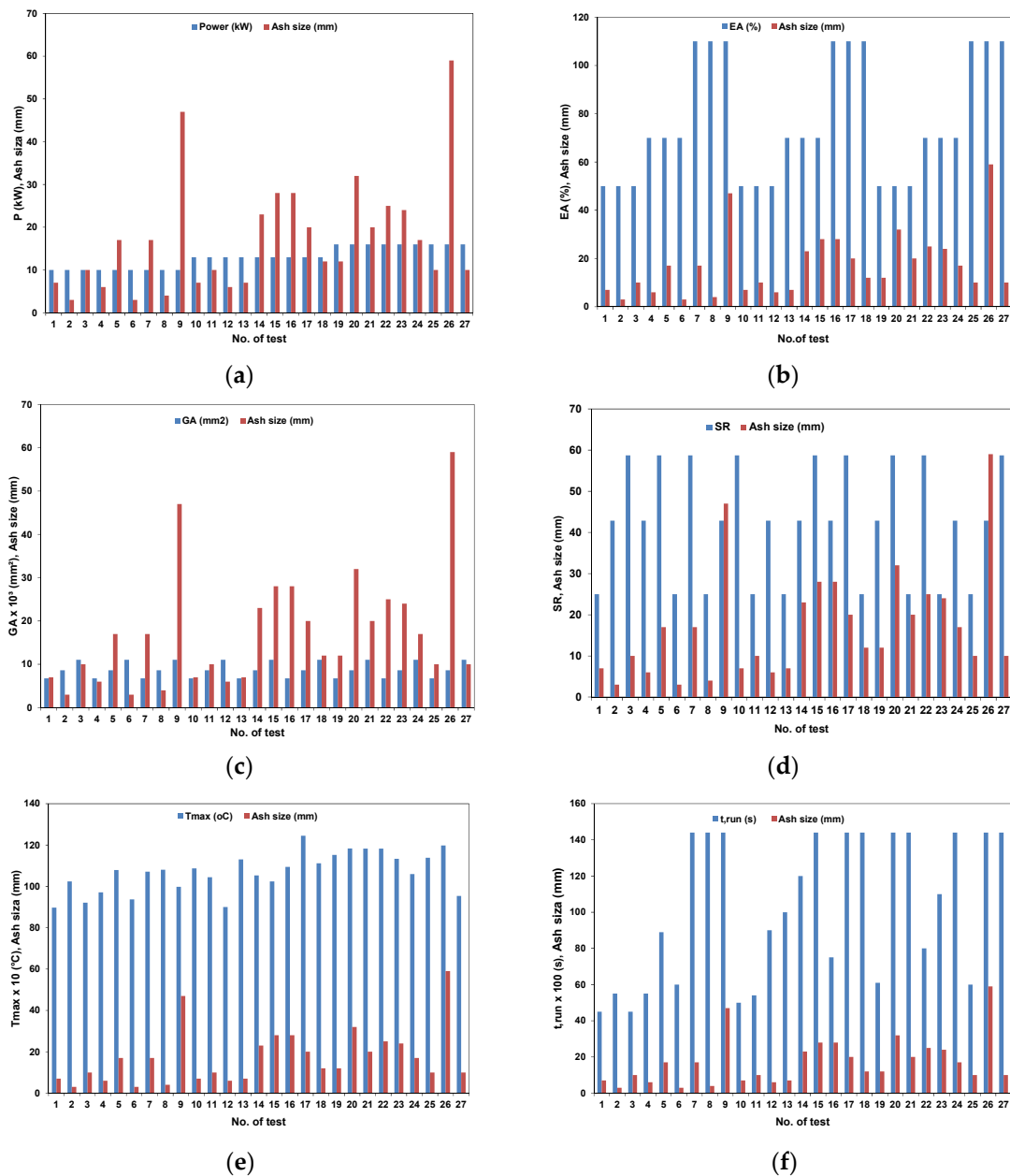


**Figure 11.** Combustion characteristics on the ashes: (a) Power (kW) vs. Ash size (mm), (b) EA (%) vs. Ash size (mm), (c) GA (mm<sup>2</sup>) vs. Ash size (mm), (d) SR vs. Ash size (mm), (e) Maximum temperature (°C) vs. Ash size (mm) and (f) Boiler running time (s) vs. Ash size (mm).

#### 4. Conclusions and Future Works

The result of this study revealed that the ash agglomerations were influenced by the duration of the combustion and the temperature of the fuel bed. The largest size of the ash agglomeration was referred to as test number-TN26 (Power of 16 kW, Excess Air 110%, Split Ratio 30/70, and Grate Area 115 mm × 75 mm), which is 59 mm, and the duration time is 14,400 s (≈4 h). This study also showed that a good combination of the parameters applied to TN9 and TN20 can be useful in obtaining stable combustion. The instability during the combustion occurs since the fuel bed rises as the accumulation of the unburned wood pellets on the grate causes the slow combustion rate and pressure drop, which creates noise and disturbances. Instability creates poor combustion, resulting in a rise in CO and possible condensation in the boiler.

The future work presented here referred to the possibility of setting up the automatic cycling period on the boiler system in order to regulate the automatic cycling method to prevent the occurrence of the instability of combustion during the combustion process, when instability occurs, in order to stabilize the combustion.

**Author Contributions:** Conceptualization, L.F.; Methodology, L.F., C.C. and P.R.; Validation, J.C.T. and E.F.; Data curation, L.F., J.C.T. and E.F.; Formal analysis: L.F., P.R. and C.C.; Investigation: L.F., P.R. and C.C.; Project Administration: J.C.T.; Resources: J.C.T. and J.M.; Writing—original draft preparation, L.F.; Writing—review and editing, L.F., P.R. and C.C.; Visualization, L.F., E.F., P.R., C.C., J.M. and J.C.T.; Supervision: J.C.T. and E.F. Project administration, J.C.T. All authors have read and agreed to the published version of the manuscript.

**Funding:** This work has been supported by FCT—Fundação para a Ciência e Tecnologia within the R&D Units, METRICS Project Scope: UIDB/04077/2020; Lelis Fraga was supported through a PhD Grant by Fundo de Desenvolvimento Capital Humano of the Government of Timor Leste.

**Data Availability Statement:** Not applicable.

**Acknowledgments:** This work is supported by FCT—Fundação para a Ciência e Tecnologia within the R&D Units Project Scope: UIDB/04077/2020 (METRICS Centre).

**Conflicts of Interest:** The authors declare no conflict of interest.

## Nomenclature

EA	Excess air
EAR	Excess Air Ratio (%)
FB	Fuel Bed
GA	Grate area (mm <sup>2</sup> )
$h$	height (mm)
$P$	Power (kW)
PM	Particular matter
RDF	Refuse derived fuel
SR	Split ratio of primary to secondary air
$T$	Temperature (°C)
$t$	Time (s)
$t_{av,ins}$	Average time of instability (h)
$T_{ex}$	Exhaust temperature (°C)
TN	Test Number
$t_{run}$	Running time (duration of the test)
XRF	X-ray Fluorescence

## References

- Garcia-Maraver, A.; Mata-Sanchez, J.; Carpio, M.; Perez-Jimenez, J.A. Critical review of predictive coefficients for biomass ash deposition tendency. *J. Energy Inst.* **2017**, *90*, 214–228. [[CrossRef](#)]
- Fang, X.; Jia, L. Experimental study on ash fusion characteristics of biomass. *Bioresour. Technol.* **2012**, *104*, 769–774. [[CrossRef](#)] [[PubMed](#)]
- Nunes, L.; Matias, J.; Catalão, J. Biomass combustion systems: A review on the physical and chemical properties of the ashes. *Renew. Sustain. Energy Rev.* **2016**, *53*, 235–242. [[CrossRef](#)]
- Magdziarz, A.; Dalai, A.K.; Koziński, J.A. Chemical composition, character and reactivity of renewable fuel ashes. *Fuel* **2016**, *176*, 135–145. [[CrossRef](#)]
- Sheng, Y.; Lam, S.S.; Wu, Y.; Ge, S.; Wu, J.; Cai, L.; Huang, Z.; Van Le, Q.; Sonne, C.; Xia, C. Enzymatic conversion of pretreated lignocellulosic biomass: A review on influence of structural changes of lignin. *Bioresour. Technol.* **2020**, *324*, 124631. [[CrossRef](#)] [[PubMed](#)]
- Ferreira, P.T.; Ferreira, M.E.; Teixeira, J.C. Analysis of Industrial Waste in Wood Pellets and Co-combustion Products. *Waste Biomass Valorization* **2014**, *5*, 637–650. [[CrossRef](#)]
- Dibdiakova, J.; Wang, L.; Li, H. Characterization of Ashes from Pinus Sylvestris forest Biomass. *Energy Procedia* **2015**, *75*, 186–191. [[CrossRef](#)]
- Rabaçal, M.; Fernandes, U.; Costa, M. Combustion and emission characteristics of a domestic boiler fired with pellets of pine, industrial wood wastes and peach stones. *Renew. Energy* **2013**, *51*, 220–226. [[CrossRef](#)]

9. Ferreira, P. Combustion of Alternative Biomass Fuels in a Domestic Boiler and in a Large-Scale Furnace. Ph.D. Thesis, University of Minho, Braga, Portugal, 2016.
10. Fraga, L.; Silva, J.; Soares, D.F.; Ferreira, M.; Teixeira, S.F.; Teixeira, J.C. Study of Devolatilization Rates of Pine Wood and Mass Loss of Wood Pellets. In Proceedings of the ASME 2017 International Mechanical Engineering Congress and Exposition, Tampa, FL, USA, 3–9 November 2017. [\[CrossRef\]](#)
11. Chlebnikovas, A.; Paliulis, D.; Kilikevičius, A.; Selech, J.; Matijošius, J.; Kilikevičienė, K.; Vainorius, D. Possibilities and Generated Emissions of Using Wood and Lignin Biofuel for Heat Production. *Energies* **2021**, *14*, 8471. [\[CrossRef\]](#)
12. Ghafghazi, S.; Sowlati, T.; Sokhansanj, S.; Bi, X.; Melin, S. Particulate matter emissions from combustion of wood in district heating applications. *Renew. Sustain. Energy Rev.* **2011**, *15*, 3019–3028. [\[CrossRef\]](#)
13. García, R.; Pizarro, C.; Álvarez, A.; Lavín, A.G.; Bueno, J.L. Study of biomass combustion wastes. *Fuel* **2015**, *148*, 152–159. [\[CrossRef\]](#)
14. Sippula, O.; Lamberg, H.; Leskinen, J.; Tissari, J.; Jokiniemi, J. Emissions and ash behavior in a 500 kW pellet boiler operated with various blends of woody biomass and peat. *Fuel* **2017**, *202*, 144–153. [\[CrossRef\]](#)
15. Olsson, M. *Residential Biomass Combustion—Emissions of Organic Compounds to Air From Wood Pellets and Other New Alternatives*; Chalmers University of Technology: Gothenburg, Sweden, 2006.
16. González, J.F.; Ledesma, B.; Alkassir, A.; González, J. Study of the influence of the composition of several biomass pellets on the drying process. *Biomass Bioenergy* **2011**, *35*, 4399–4406. [\[CrossRef\]](#)
17. Vicente, E.; Duarte, M.; Calvo, A.; Nunes, T.; Tarelho, L.; Custódio, D.; Colombi, C.; Gianelle, V.; de la Campa, A.S.; Alves, C. Influence of operating conditions on chemical composition of particulate matter emissions from residential combustion. *Atmos. Res.* **2015**, *166*, 92–100. [\[CrossRef\]](#)
18. Toscano, G.; Corinaldesi, F. Ash fusibility characteristics of some biomass feedstocks and examination of the effects of inorganic additives. *J. Agric. Eng.* **2010**, *41*, 13–19. [\[CrossRef\]](#)
19. Tortosa-Masiá, A.; Ahnert, F.; Spliethoff, H.; Loux, C.; Hein, K. Slagging and fouling in biomass co-combustion. *Therm. Sci.* **2005**, *9*, 85–98. [\[CrossRef\]](#)
20. Lin, Q.; Tay, K.L.; Yu, W.; Zong, Y.; Yang, W.; Rivellini, L.-H.; Ma, M.; Lee, A.K.Y. Polyoxymethylene dimethyl ether 3 (PODE3) as an alternative fuel to reduce aerosol pollution. *J. Clean. Prod.* **2020**, *285*, 124857. [\[CrossRef\]](#)
21. Wang, L.; Hustad, J.E.; Skreiberg, Ø.; Skjevrak, G.; Grønli, M. A Critical Review on Additives to Reduce Ash Related Operation Problems in Biomass Combustion Applications. *Energy Procedia* **2012**, *20*, 20–29. [\[CrossRef\]](#)
22. Wang, Y.; Tan, H.; Wang, X.; Du, W.; Mikulčić, H.; Duić, N. Study on extracting available salt from straw/woody biomass ashes and predicting its slagging/fouling tendency. *J. Clean. Prod.* **2017**, *155*, 164–171. [\[CrossRef\]](#)
23. Wang, Y.; Shao, Y.; Matovic, M.D.; Whalen, J.K. Exploring switchgrass and hardwood combustion on excess air and ash fouling/slagging potential: Laboratory combustion test and thermogravimetric kinetic analysis. *Energy Convers. Manag.* **2015**, *97*, 409–419. [\[CrossRef\]](#)
24. Wiinikka, H.; Gebart, R. Critical Parameters for Particle Emissions in Small-Scale Fixed-Bed Combustion of Wood Pellets. *Energy Fuels* **2004**, *18*, 897–907. [\[CrossRef\]](#)
25. Öhman, M.; Boman, C.; Hedman, H.; Nordin, A.; Boström, D. Slagging tendencies of wood pellet ash during combustion in residential pellet burners. *Biomass Bioenergy* **2004**, *27*, 585–596. [\[CrossRef\]](#)
26. Verma, V.; Bram, S.; Delattin, F.; De Ruyck, J. Real life performance of domestic pellet boiler technologies as a function of operational loads: A case study of Belgium. *Appl. Energy* **2013**, *101*, 357–362. [\[CrossRef\]](#)
27. Xiao, R.; Chen, X.; Wang, F.; Yu, G. The physicochemical properties of different biomass ashes at different ashing temperature. *Renew. Energy* **2011**, *36*, 244–249. [\[CrossRef\]](#)
28. Fachinger, F.; Drewnick, F.; Gieré, R.; Borrmann, S. How the user can influence particulate emissions from residential wood and pellet stoves: Emission factors for different fuels and burning conditions. *Atmos. Environ.* **2017**, *158*, 216–226. [\[CrossRef\]](#)
29. Biryukov, V.I. *Bases of Combustion Instability. Direct Numerical Simulations—An Introduction and Applications*; IntechOpen: London, UK, 2021. [\[CrossRef\]](#)
30. Yoon, M. Combustion instability analysis from the perspective of acoustic impedance. *J. Sound Vib.* **2020**, *483*, 115500. [\[CrossRef\]](#)
31. Annaswamy, A.; Ghoniem, A. Active control of combustion instability: Theory and practice. *IEEE Control Syst.* **2002**, *22*, 37–54. [\[CrossRef\]](#)
32. Castro, C.; Fraga, L.; Ferreira, E.; Martins, J.; Ribeiro, P.; Teixeira, J.C. Experimental Studies on Wood Pellets Combustion in a Fixed Bed Combustor Using Taguchi Method. *Fuels* **2021**, *2*, 376–392. [\[CrossRef\]](#)
33. European Pellet Council. ENplus Handbook CANADA, Part 3: Pellet Quality Requirements, Quality Certification Scheme for Wood Pellets. Version 3.0, August, 2015. Available online: <https://enplus-pellets.eu/en-ca/component/attachments/?task=download&id=544> (accessed on 2 August 2023).
34. Ribeiro, P.E.A. Aglomeração de Cinzas numa Caldeira a Pellets—Influência da Temperatura e do Fluxo de Ar. Master's Thesis, University of Minho, Braga, Portugal, 2012.
35. Klason, T.; Bai, X. Computational study of the combustion process and NO formation in a small-scale wood pellet furnace. *Fuel* **2007**, *86*, 1465–1474. [\[CrossRef\]](#)

36. Kraiem, N.; Lajili, M.; Limousy, L.; Said, R.; Jeguirim, M. Energy recovery from Tunisian agri-food wastes: Evaluation of combustion performance and emissions characteristics of green pellets prepared from tomato residues and grape marc. *Energy* **2016**, *107*, 409–418. [[CrossRef](#)]
37. Yazdanpanah, F.; Sokhansanj, S.; Lau, A.; Lim, C.; Bi, X.; Melin, S. Airflow versus pressure drop for bulk wood pellets. *Biomass Bioenergy* **2011**, *35*, 1960–1966. [[CrossRef](#)]
38. Ray, S.J.; Pordesimo, L.O.; Wilhelm, L.R.; Buschermohle, M.J. Airflow Resistance of Some Pelleted Feed. In Proceedings of the 2003 ASAE Annual Meeting, Las Vegas, NV, USA, 27–30 July 2003. [[CrossRef](#)]
39. Roy, M.M.; Dutta, A.; Corscadden, K. An experimental study of combustion and emissions of biomass pellets in a prototype pellet furnace. *Appl. Energy* **2013**, *108*, 298–307. [[CrossRef](#)]
40. Fraga, L.G.; Silva, J.; Teixeira, J.C.; Ferreira, M.E.C.; Teixeira, S.F.; Vilarinho, C.; Gonçalves, M.M. Study of Mass Loss and Elemental Analysis of Pine Wood Pellets in a Small-Scale Reactor. *Energies* **2022**, *15*, 5253. [[CrossRef](#)]
41. Öhman, M.; Nordin, A.; Hedman, H.; Jirjis, R. Reasons for slagging during stemwood pellet combustion and some measures for prevention. *Biomass Bioenergy* **2004**, *27*, 597–605. [[CrossRef](#)]
42. Ribeiro, P.; Teixeira, J.; Ferreira, M.E. Ash Sintering in a Biomass Pellet Boiler. In Proceedings of the ASME 2013 International Mechanical Engineering Congress and Exposition, San Diego, CA, USA, 15–21 November 2013; Volume 8A, pp. 1–7. [[CrossRef](#)]

**Disclaimer/Publisher’s Note:** The statements, opinions and data contained in all publications are solely those of the individual author(s) and contributor(s) and not of MDPI and/or the editor(s). MDPI and/or the editor(s) disclaim responsibility for any injury to people or property resulting from any ideas, methods, instructions or products referred to in the content.